

Chapter 1

Introduction

Economic and societal setup of India depends primarily on the crop yield, which in turn is decided by the variability in monsoon rain. Severe draught or flood events when persistent for a long period of time, may lead to country wide devastation. Since Indian Summer Monsoon (ISM) contributes to $\sim 80\%$ of the annual rainfall in India, the economy of the country critically depends upon the performance of the monsoon [[Gadgil, 2003](#)].

Understanding the causative processes affecting rainfall occurrences requires continuous instrument based monitoring and observations of meteorological parameters, and in parallel development of mathematical models validated by the observations. We also need to look into the variability and conditions of Earth's climate in the near and also distant past. This is part of a discipline known as paleoclimatology, which is the study of past or ancient climates.

1.1 Indian Summer Monsoon

The word monsoon is derived from the Arabic word “mausam” which is defined as seasonal reversal of winds. It has been suggested that monsoon system was established about 20 million years ago due to the uplift of the Tibetan plateau. Indian Summer Monsoon (ISM) is a manifestation of the seasonal migration of

the Inter-tropical Convergence Zone (ITCZ, [Gadgil, 2003]) in response to heating of the high altitude Tibetan plateau (Figure 1.1). ITCZ is the region where trade winds merge together and form a low pressure belt. During the northern summer, the Indian subcontinent gets heated up and a low pressure trough is formed. This heat induced low pressure (<999 mb) extends from northern Rajasthan to Kolkata at the surface level. Concomitantly, Austral winter causes high pressure over the southern hemispheric subtropical Indian ocean ($\sim 30^{\circ}\text{S}$), also known as the Mascarene High (>1023 mb). This pressure gradient drives cross equatorial flow of heat and moisture. On account of this, the ITCZ migrates over the Indian region causing the wind flow from the southwest leading to monsoon precipitation [Gadgil, 2003; Sikka and Gadgil, 1980]. Shift of ITCZ is a climate system behavior occurring at a global scale and hence Indian monsoon forms an interactive part of the global monsoon system. However, ITCZ behavior on local and regional scales is quite complex [Tomas and Webster, 1997], and hence unique to a particular geographic setting.

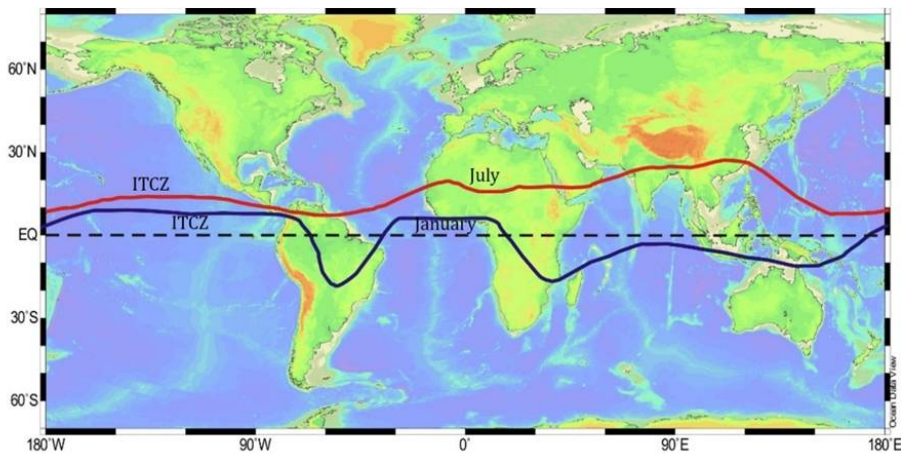


Figure 1.1: Equatorial position of ITCZ in January (blue) and its northward migration in July (red). Re-drawn from: *The Atmosphere* [Lutgens and Tarbuck, 2000], using ocean data viewer.

The Indian monsoon generally responds to interglacial/glacial events by intensification/weakening of its strength.

1.1.1 Variability

Strength of ISM varies on different timescales ranging from intraseasonal to interannual, decadal, centennial and millennial [e.g., [Gadgil, 2003](#); [Ramesh et al., 2010](#)]. The intraseasonal oscillation reflected as active and break cycles of monsoon, [[Rajeevan et al., 2010](#)] having 30-60 day oscillations, are mainly controlled by the internal dynamics. The interannual variability of monsoon rainfall is mainly governed by both the internal dynamics as well as the external controls such as El Niño Southern Oscillation (ENSO) [[Kumar et al., 1999](#)], the solar cycle etc. The longer time scale variability (decadal to millennial) is controlled by the changes in incoming solar radiation (insolation) associated with changes in the Earth's orbital parameters along with the changes in circulation pattern [[Imbrie and Imbrie, 1986](#)].

1.1.2 Paleo-monsoon reconstruction

Instrumental record of monsoon rainfall exists for the past 100 or 150 years and historical records gives qualitative estimates for a few hundred years farther back in time. Long term reconstruction of monsoon necessitates exploiting natural archives which preserve signatures of the monsoon in the form of faunal and floral counts, characteristic chemical constituents and isotopic compositions. The most widely used and accepted archives are tree rings [e.g., [Managave et al., 2011b](#); [Ramesh et al., 1989](#); [Sano et al., 2010](#)], speleothems [e.g., [Allu et al., 2015](#); [Laskar et al., 2011](#); [Ramesh et al., 2010](#); [Sinha et al., 2007](#); [Yadava and Ramesh, 1999, 2001, 2005, 2006](#); [Yadava et al., 2004](#)], lake sediments [e.g., [Enzel et al., 1999](#); [Prasad and Enzel, 2006](#)] and river sediments [e.g., [Juyal et al., 2006](#); [Khadkikar et al., 2000](#); [Sridhar et al., 2016](#)], and ocean sediments [e.g., [Gupta et al., 2003](#); [Kudrass et al., 2001](#); [Prabhu et al., 2004](#)]. Each of these archives have associated advantages and drawbacks. Tree rings with sub-annual resolution have the limitation of the extent of time to which they are available. Ocean sediments

on the other hand, preserve longer timescale climatic data but lack the ability to reconstruct annual or decadal monsoonal variability. However, in the case of speleothems using the U-Th dating technique, potential ISM variability for past 500,000 years can be reconstructed. Also, a speleothem grown under favorable conditions may offer annual resolution.

1.2 Stable isotopologues of carbon dioxide

Different combinations of the isotopes form CO_2 molecules with different masses, called CO_2 isotopologues. Carbon dioxide isotopologues constitute mainly three masses, with the most abundant mass of 44, CO_2 containing ^{13}C atom of mass 45, and additionally, CO_2 containing an ^{18}O instead of the ^{16}O oxygen isotope has mass 46. There are a few CO_2 molecules with a ^{13}C and a ^{18}O , or two atoms of ^{18}O with very low abundances. The three major isotopologues of CO_2 with their relative abundance are shown in table 1.1.

Table 1.1: *Isotopologues of carbon dioxide along with their natural abundances. Source: National Oceanic and Atmospheric Administration (NOAA)*

Mass	Isotopologues	Abundance (%)
44	$^{12}C^{16}O_2$	98.40
45	$^{13}C^{16}O_2$	1.19
	$^{12}C^{17}O^{16}O$	0.0748
46	$^{12}C^{18}O^{16}O$	0.41
	$^{13}C^{17}O^{16}O$	0.00084
	$^{12}C^{17}O_2$	0.0000142

As seen above masses 45 and 46 include $^{12}C^{17}O^{16}O$ and $^{13}C^{17}O^{16}O$, $^{12}C^{17}O_2$ respectively, with very low abundances. However, for paleoclimate studies, importance is given to relative abundance of ^{13}C and ^{18}O isotopes. Hence, Craig correction is applied to negate the effect of the former low abundant masses [[Craig, 1957](#)].

1.2.1 Notations

The relative abundance of any heavier isotope is conveniently represented as it's ratio with that of the lighter one.

$$R = \frac{\text{Abundance of the heavier isotope}}{\text{Abundance of the lighter isotope}}$$

As the absolute ratios of the isotopes are difficult to measure and the relative variations are of principal interest in understanding a process, isotopic ratios are expressed as deviations (δ) from that of an international standard. Carbon dioxide isotopic compositions are reported with respect to the standard procured from International Atomic Energy Agency (IAEA): Vienna Pee Dee Belemnite (VPDB)[[Gonfiantini, 1978](#); [Gonfiantini et al., 1995](#)]. For example, carbon-13 and oxygen-18 abundances in a sample are reported respectively as

$$\delta^{13}C = \left(\frac{R_{Sample}}{R_{Standard}} - 1 \right) \times 10^3\text{‰}$$

and

$$\delta^{18}O = \left(\frac{R_{Sample}}{R_{Standard}} - 1 \right) \times 10^3\text{‰},$$

1.2.2 Isotopic Fractionation of CO_2 in soil

When the infiltrating water dissolves soil CO_2 , some of it hydrates and dissociates to form bicarbonate (HCO_3^-) and carbonate (CO_3^{2-}) ions. The concentrations of these species at any given time is controlled by the pH of the local meteoric water. At each step of ion formation different fractionation factors are involved and the largest fractionation occurs during CO_2 hydration (Figure 1.2). The rate of fractionation also depends upon closed and open system conditions (explained in detail in chapter 2), and type of parent material. In silicate bedrock terrains,

there is less presence of Dissolved Inorganic Carbon (DIC) evolution, whereas in carbonate bedrock terrains, dissolution of calcite/dolomite acts as an additional source of carbon to the DIC pool.

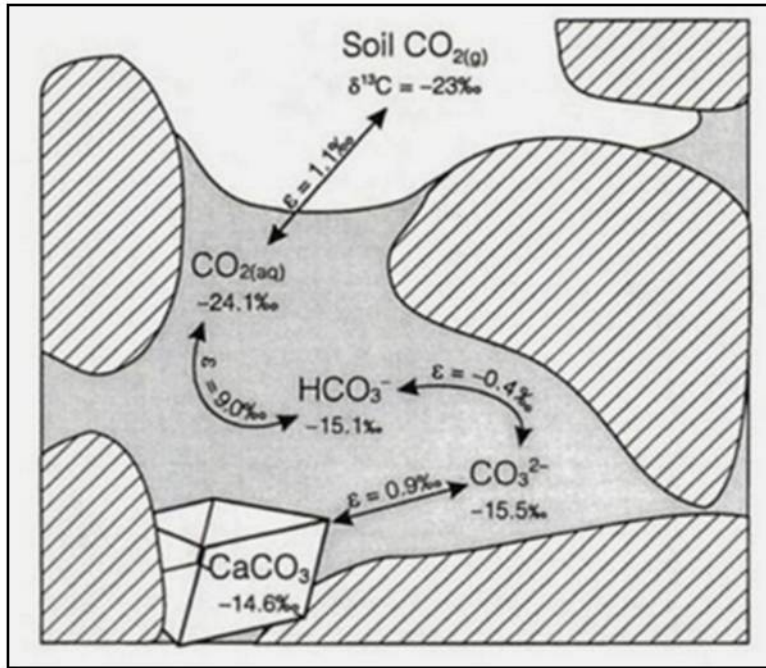


Figure 1.2: Schematic of fractionation of ^{13}C in during equilibrium exchange of carbon between CO_2 , Dissolved Inorganic Carbon and calcite at 25°C . Source: Clark and Fritz [1997]

1.2.3 Rayleigh model for isotopic fractionation

The isotopic composition of a system from which material is continuously removed can be studied using the Rayleigh model [Mook, 2006]. Consider a reservoir (vapor mass) from which rain is continuously removed by condensation. On account of isotopic fractionation, the remanant vapor gets depleted in ^{18}O and the rain is enriched in ^{18}O . The following assumptions are important, i) the abundance of heavier isotopes is much less than that of the lighter ($N^* \ll N$), ii) the isotopic fractionation occurs with instantaneous isotopic equilibrium, iii) the process is isothermal and iv) the reservoir is homogeneous (no isotopic gradient across the reservoir). At any instant, the stable isotope ratio R of the vapour is

given by

$$R = \frac{N^*}{N},$$

where N^* and N are the number of heavier and lighter isotopologues. Differentiating the equation gives,

$$dR = \frac{dN^*}{N} - \frac{RdN}{N}$$

By solving the equation with fractionation factor $\alpha = \frac{dN^*}{dN}/R$, we get

$$R = R_0 f^{\alpha-1}$$

Where, R_0 is the initial isotopic ratio of vapor and f is the fraction of substance remaining in the reservoir. In δ notations, Rayleigh equation can be expressed as

$$\delta = \delta_0 + (\alpha - 1)10^3 \ln f$$

The variation of isotopic composition of the water vapour, rain and the accumulated rain formed from the vapour at any instant according to the Rayleigh fractionation are shown in Fig 1.3 [Clark and Fritz, 1997]. In permil notation α is represented as the separation factor,

$$\epsilon = (\alpha - 1).10^3\text{‰}$$

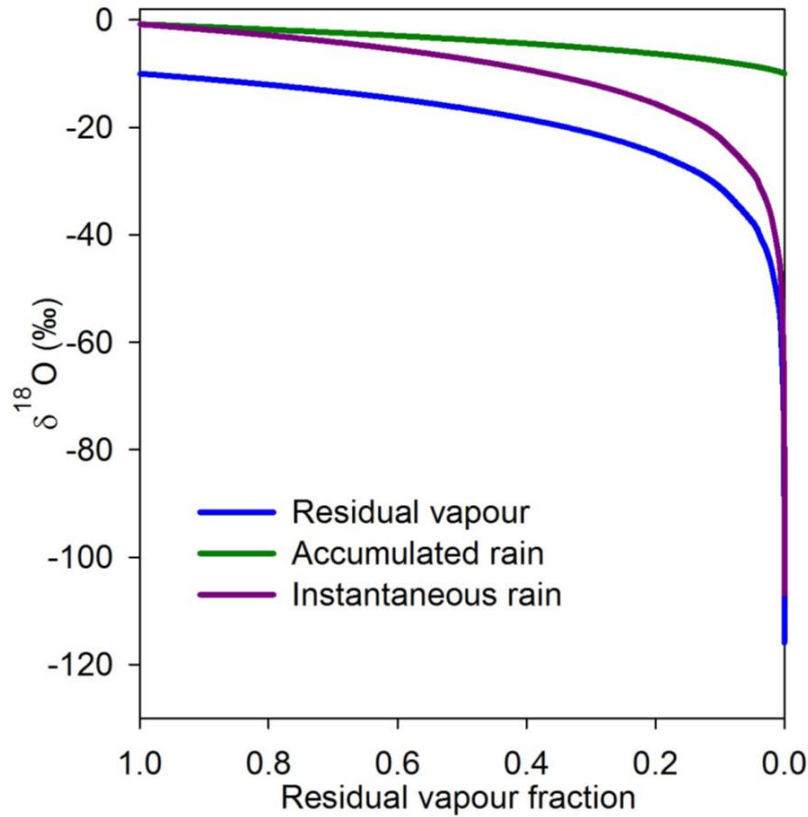


Figure 1.3: The change in the $\delta^{18}\text{O}$ of the water vapor, instantaneous rain and the accumulated rain formed from the water vapor versus the fraction of vapour remaining in the system. The process follows Rayleigh isotopic distillation. Figure redrawn from *Lekshmy [2015]*.

1.2.4 Observed isotopic effects

Stable isotopes of global precipitation shows large variations due to isotopic effects and geography.

1. **Temperature effect:** Temperature effect is the observed linear relationship between the mean annual surface air temperature and the mean annual precipitation isotopic composition (Figure 1.4). The relationship is based on the data procured from the Global Network of Isotopes in Precipitation (GNIP) and the mean annual air temperature at each station [e.g., *Dansgaard, 1964; Rozanski et al., 1993*],

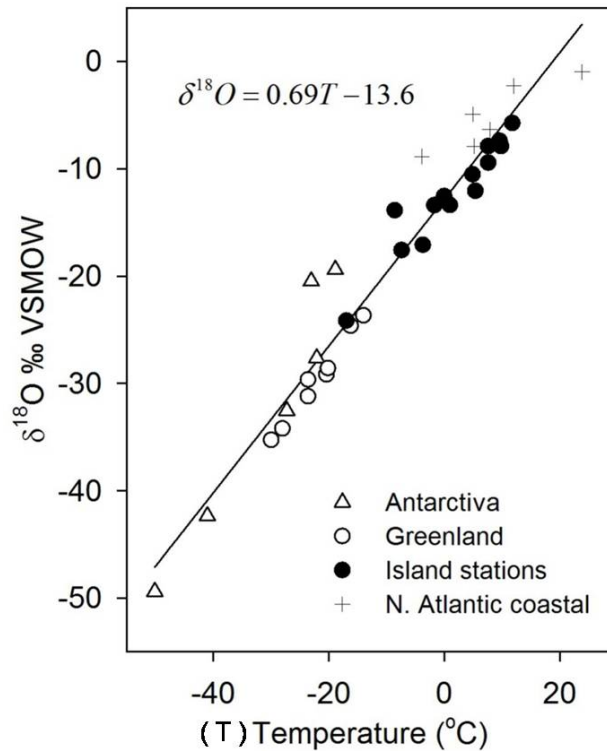


Figure 1.4: Temperature- $\delta^{18}O$ relationship in precipitation in Antarctica, Greenland, Island stations and N. Atlantic coastal. [source: [Clark and Fritz, 1997](#)]

$$\delta^{18}O = 0.695T_{annual} - 13.6$$

$$\text{‰}\delta D = 5.6T_{annual} - 100\text{‰}$$

This is obeyed mainly by high latitude precipitation and does not apply to tropical rain.

2. **Amount effect:** The explained temperature effect is predominately observed at high latitudes, especially where the mean annual surface air temperature is $> 15^{\circ}\text{C}$. In tropics, the isotopic composition of precipitation is controlled by the amount of rainfall. This phenomenon is known as "amount effect" [[Dansgaard, 1964](#)]. It is defined as the negative relation between the

precipitation isotopic ratio and rainfall [Fig 1.5]. [Dansgaard \[1964\]](#) observed $-1.5 \text{‰}/100 \text{ mm}$ of monthly rain on 14 islands distributed at tropical latitudes. The factors responsible for amount effect are :i) according to the Rayleigh isotopic fractionation, the newly formed condensate is enriched in ^{18}O .ii) There is re-evaporation of isotopically lighter rain at the bottom of the cloud because of lower humidity.

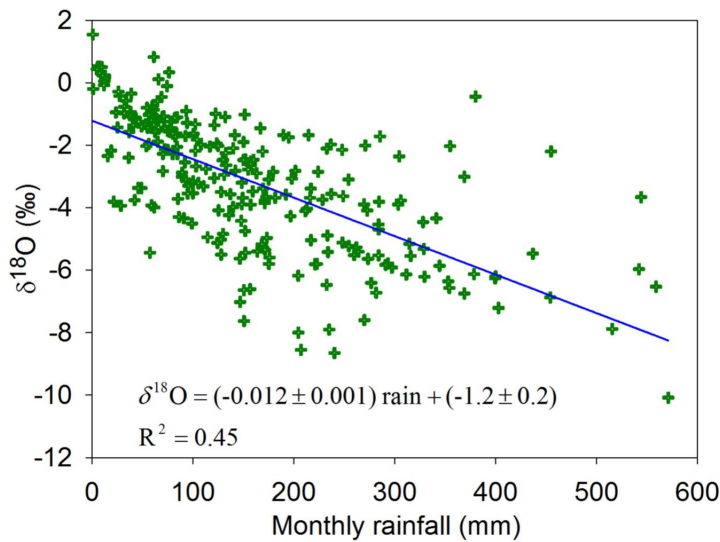


Figure 1.5: Relation between monthly rainfall and its $\delta^{18}\text{O}$ in tropical island stations around the globe [source: GNIP data, [\[Lekshmy, 2015\]](#)].

This exchanges isotopes with rain drops. So higher rainfall (high humidity) reduces the ^{18}O in rain. However, the process controlling the amount effect needs further investigation.

In the tropics, atmospheric convection is the main source of precipitation. Figure 1.6 shows a schematic representation of different components of a convective cloud system. The moisture feeding the system is derived from sub-cloud layer (SL), which consists of the surface evaporation, recycled moisture from the cloud and the entrained environmental moisture. In

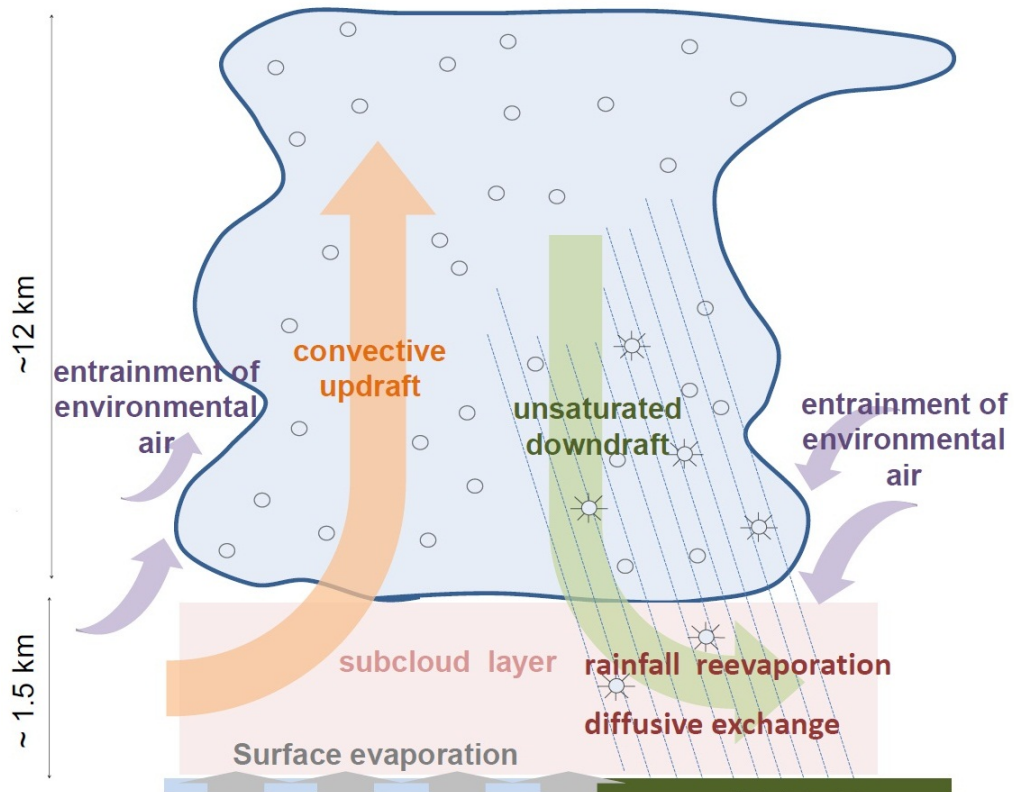


Figure 1.6: Schematic representation of a convective cloud system Source: [Lekshmy, 2015; Risi et al., 2008].

case of intense convection, high SL vapor is taken into the cloud in addition to entrained environmental air which is more depleted in the heavier isotopes. ^{18}O and D depleted water vapor (unsaturated) is formed due to condensation inside the cloud, that reaches the SL by downdraft. The re-evaporation of the rain drops also feed isotopically depleted vapor to the SL vapor. Hence, during strong convection, effective recycling of the moisture leads to depleted of ^{18}O and D of rainfall [Lekshmy, 2015; Risi et al., 2008]

- 3. The altitude effect:** As the vapor mass ascends over a mountain and cools down adiabatically, it leads to orographic precipitation. Precipitation starting at a particular height of the mountain continues till the top. Continuous precipitation leads to enriched ^{18}O and D rain at lower altitude

and depleted values at higher altitude. This process known as the altitude effect (negative relation between $\delta^{18}O$ and δD of rain and altitude) as seen in Figure 1.7.

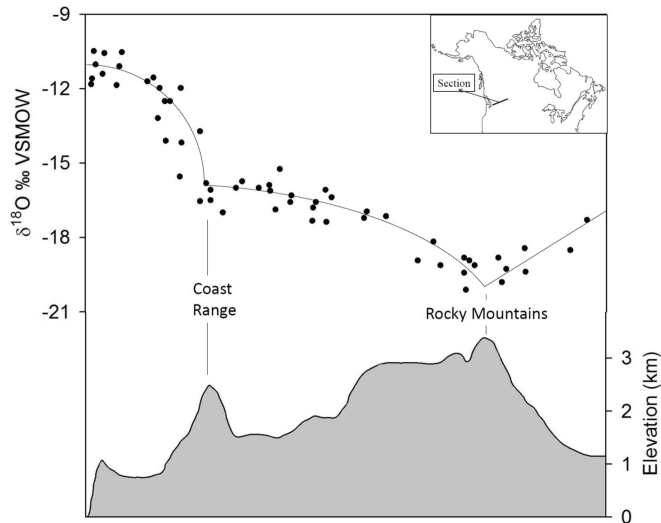


Figure 1.7: $\delta^{18}O$ variation along a high altitude mountain region [source: *Yonge et al., 1989*].

4. The continental effect:

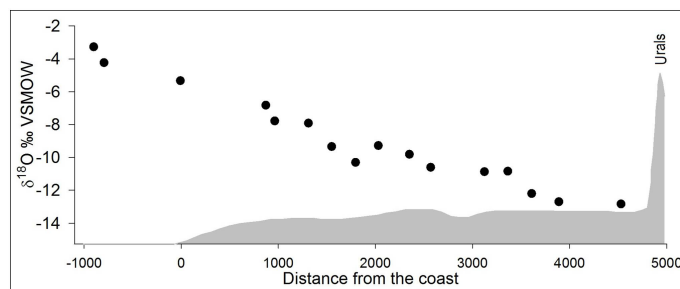


Figure 1.8: Variation of $\delta^{18}O$ from oceanic (southwest coast of Ireland) to inland region (Perm) over Europe [source: *Rozanski et al., 1993*].

The vapor mass transporting from its source region to inland, continues to rain out leading to the preferential removal of the heavier isotope in the initial rainout. The gradual depletion of the heavier isotopes is observed in

the precipitation as the vapor mass travels to the interior of the continents. This effect is known as the continental effect. Figure 1.8 shows an example of continental effect on the long term annual $\delta^{18}O$ of precipitation in Europe.

1.3 Objectives

Variability of ISM throughout the Holocene has been a debatable issue. While some workers showed that monsoon decreased in response to decline in insolation, others infer that gradual increase in its intensity from 11.7 ka to present. There is another growing consensus about the trend of decrease in monsoon during mid-Holocene which faced widespread aridification with prolonged droughts. The schools of thought are divided between abrupt or gradual decline of monsoon during mid-Holocene. Hence, the focus of the present work is to address the following issues:

1. To generate high resolution speleothem $\delta^{18}O$ record covering the entire Holocene.
2. To test the concepts of increase or decrease in monsoon throughout the Holocene.
3. To test for coherence between speleothem based monsoon reconstructions and other proxy records.
4. To assess the contributions of various internal and external driving forces in governing millennial and centennial monsoon oscillations.

Understanding the variability of monsoon on glacial-interglacial timescales is equally important as studying Holocene ISM changes. The longer records of reconstructed ISM show that it was stronger during interglacial and weaker during glacial periods [*Sirocko et al., 1993*], whereas the winter monsoon was stronger during glacial periods. Hence part of this thesis work focuses on :

1. To verify the response of ISM on glacial-interglacial timescales.
2. To study the role of insolation in driving the monsoon variability.
3. To identify the primary drivers of the monsoon system on glacial-interglacial climate oscillations.

The aforementioned issues are addressed using the five stalagmite samples and a sediment core from Andaman Sea. Three of these samples are used to study the Holocene variability of monsoon and the other two are used to reconstruct paleomonsoon during the late Pleistocene.

1.4 Previous work

Use of speleothem as a proxy to reconstruct the Indian Monsoon, is quite well established [[Kotlia et al., 2014](#); [Laskar et al., 2013](#); [Lone et al., 2014](#); [Sanwal et al., 2013](#); [Yadava and Ramesh, 2005, 2006](#); [Yadava et al., 2004](#)]. In India, speleothem formations are found where there are large outcrops of limestone bedrocks. Cluster of caves are found in Kanger valley National park, Chattisgarh. As this area falls in the core monsoon region of India, speleothems formed here represent changes in the amount of monsoon precipitation. Several studies have been carried out on speleothems from these caves [[Ramesh et al., 2010](#); [Sinha et al., 2007](#); [Yadava and Ramesh, 2006](#)]. Monsoon variability during 14th and 15th century is captured in a 900 years (600-1500 AD) old stalagmite from Dandak cave. Major famines like Durga Devi famine that lasted from 1396 -1409 AD during ‘Little Ice Age’ coincides with the enriched oxygen values of speleothem of this timespan. Higher precipitation during ‘Medieval warming’ during 900-1350 AD is also recorded in the stalagmite. Variability of monsoon during Little ice age and Medieval warming is correlated with change in the solar activity [[Sinha et al., 2007](#)].

Based on the 3400 yr BP old Gupteshar stalactite sample it was inferred that high rainfall persisted from 3400-2900 yr BP with declining monsoon intensity during 2900-1200 yr BP. Since then increase in precipitation was recorded till present [*Yadava and Ramesh, 2005, 2006; Yadava et al., 2004*]. Speleothems formed elsewhere in India are also used for monsoon reconstruction. A 331 year old stalagmite, from the Akalagavi cave of Northern Karnataka, India, revealed distinct annual layers. Variability in the monsoon rain during CE 1650-1997, with the highest precipitation at CE 1666 and the lowest around CE 1900 [*Yadava et al., 2004*] was observed. *Laskar et al. [2011, 2013]*, studied a stalagmite from Baratang cave, Andaman to assess the potential of the Andaman speleothems as monsoon recorders. Weaker ISM was observed during Roman Warm Period (2100 - 1800 cal BP) while strong ISM observed during Medieval warming. Another stalagmite sample from the Valmiki cave, southern India covering a time span of 15,700 to 14,700 a (U-Th dated) was used to infer abrupt changes in monsoon rain during the last deglaciation [*Lone et al., 2014*]. Another study from Mawmulah cave, Meghalaya records an ISM variability from 33.8 - 5.5 ka [*Dutt et al., 2015*]. Abrupt increase in rainfall during Bolling-Allerod and early Holocene and significant weakening during Younger Dryas and Heinrich cold event was observed. Solar forcing and strong ocean-atmospheric circulation were suggested as possible controllers of the ISM dynamics [*Allu et al., 2015; Asmerom et al., 2013*]. The work in this field is growing with new stalagmite studies carried across India. Many more caves are explored to assess their potential for paleoclimatic studies.